

## Avinash Gudimetla<sup>1\*</sup>, Dumpla Lingaraju<sup>2</sup>, S. Sambhu Prasad<sup>3</sup>

<sup>1</sup> Research Scholar, Department of Mechanical Engineering, JNTUK, Kakinada, Andhra Pradesh, India

<sup>2</sup> Department of Mechanical Engineering, University College of Engineering, JNTUK, Kakinada, Andhra Pradesh, India

<sup>1,3</sup> Department of Mechanical Engineering, Pragati Engineering College, Surampalem, Andhra Pradesh, India

\*Corresponding author. E-mail: avinashdattu1@gmail.com

Received (Otrzymano) 7.02.2021

# MODELLING AND OPTIMIZATION OF WEAR PARAMETERS OF Al 4032 REINFORCED WITH COAL ASH USING TAGUCHI AND RSM APPROACH

The present study aimed to analyze the wear behaviour of composites synthesized by reinforcing Al 4032 with 2, 4, 6 wt.% of coal ash using the stir casting technique. Wear testing was performed on the composites at room temperature in the absence of lubrication using a pin-on-disc tribometer considering the process parameters as wt.% of reinforcement, speed and load. Micro structural characterization using scanning electron microscope (SEM) and energy dispersive X-ray analysis (EDX) was performed on the cast composites to ascertain the existence of the reinforcement along with its distribution in the prepared composites. The Taguchi L<sub>16</sub> orthogonal array was utilized to design experiments to study the significance of the process parameters on the wear rate. A mathematical model was developed for the wear rate using response surface methodology (RSM). 6 wt.% reinforcement, at the speed of 100 rpm and 10 N load were the obtained optimized parameters for the minimum wear rate. Surface plots as well as contour plots were analyzed to understand the consequence of the process parameters on the wear rate. The analysis of variance (ANOVA) revealed that speed with 76.10 % was the most prominent parameter followed by load and reinforcement with 11.23 and 9.42% respectively.

**Keywords:** coal ash, stir casting, mechanical properties, wear rate, Taguchi, RSM, ANOVA

## INTRODUCTION

Enhancement of the mechanical properties along with better tribological characteristics can be obtained by tailor-made materials by reinforcing metal matrices with micro-sized particulates, which find applications in many verticals of engineering, industry, recreation and many more [1-3]. The research on aluminium is increasing because of its distinguished features of low cost, light weight and better mechanical properties [4-6] along with its ability to be cast with various types of reinforcement [7], which have made aluminium a promising material with high strength and stiffness in various structural applications. Few studies have been performed on Al 4032 [2, 8] and by considering its importance in the automobile industry and other fields [9], it was chosen as the matrix material in this study.

Different types of materials like particulates and fibers [7] are employed to reinforce aluminium in order to enhance its wear resistance along with its strength. Better tribological characteristics were obtained by reinforcing aluminium metal matrices with particulates when compared with unreinforced aluminium and its alloys [10]. Research on aluminium alloys was conducted by reinforcing them with various ceramic particles and better wear resistance was reported by researchers [11-17]. The uses of hybrid reinforcements

have also shown a promising increase in mechanical and wear characteristics, because of the embodiment of hard reinforcements, which contributed to the increase in hardness of the composites [18].

A by-product from thermal power plants is coal ash, which was chosen as the reinforcement in the present study to investigate its effect on the wear characteristics of Al 4032. Some authors have reported the use of ash as reinforcement, which enhanced the hardness and mechanical properties of composites [19-21]. Reinforcing Al 4032 with coal ash reduces the problems associated with the disposal of industrial waste from thermal power plants, making the environment pollution free as well as fabrication of low-density composites at a low cost, with better mechanical and wear characteristics.

There are many methods for fabricating composites as reported by authors [22-32]. Stir casting is one of the low-cost techniques for fabricating composites with better distribution of the reinforcement, leading to better strength of composites. Hence, in this study, stir casting was used to fabricate composites with coal ash as reinforcement.

The design of experiments (DOE) is an abundantly used statistical tool to study the effect of process parameters on responses with a minimum number of

experiments, leading to a reduction in the time and costs associated with conducting experiments. Various orthogonal arrays proposed by Taguchi have been utilized by authors to successfully understand the effect of process parameters on responses [33-38]. The design of experiments was carried out as per the Taguchi  $L_{16}$  orthogonal array. Furthermore, RSM was used to develop a mathematical model for the wear rate and to optimize the process parameters for the minimum wear rate.

## EXPERIMENTATION PROCEDURE

### Composite synthesis

Al 4032 was procured from a leading supplier and was cut in to small pieces so as to feed it easily into the crucible and its chemical composition is given in Table 1.

TABLE 1. Composition of Al 4032

Element	Al	Si	Cu	Mg	Ni	Fe
wt.%	83.78	13.2	1.0	1.1	0.9	0.02

TABLE 2. Composition of coal ash

Element	O	Al	Si	K	Ti	Fe
wt.%	50.63	18.1	26.28	1.08	1.06	2.86

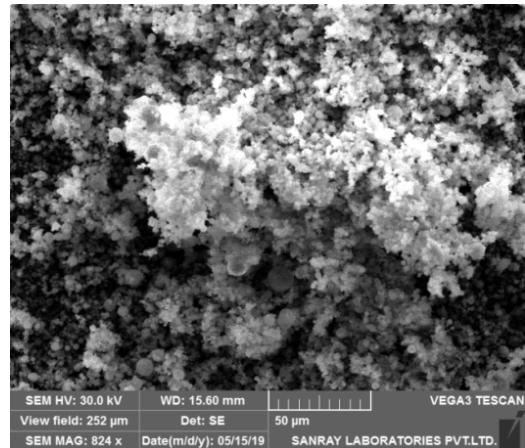


Fig. 1. SEM image of coal ash

Coal ash was collected from a thermal power plant and sieved to obtain reinforcement of an average size less than or equal to 50  $\mu\text{m}$ . The chemical composition of the coal ash is given in Table 2. An SEM micrograph of coal ash is shown in Figure 1 and the particulars of the material are given in Table 3.

TABLE 3. Particulars of coal ash

Reinforcement	Average grain size [ $\mu\text{m}$ ]	Density [ $\text{g}/\text{cm}^3$ ]	[wt.%]
Coal ash	50	1.032	2,4,6

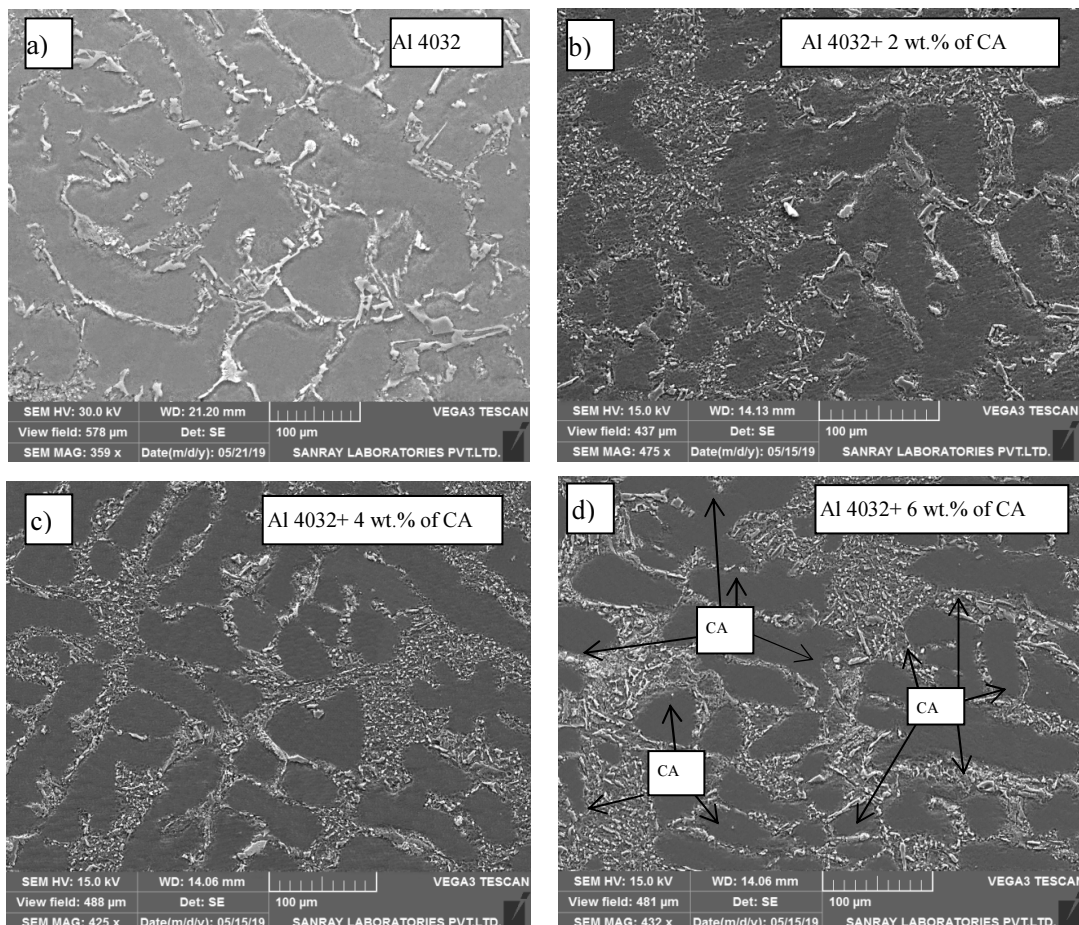


Fig. 2. SEM micrographs of Al 4032 and composites with 2, 4, 6 wt.% of coal ash (a-d)

The stir casting technique was chosen to fabricate the composites. A muffle furnace with a heating range of 1100°C was chosen for the fabrication and it was kept in the vertical position. A stirrer with provision for varying its height was made to stir the liquid metal at the required heights. The coal ash that was used as the reinforcement was collected from the power plant at stage 10 of the electro static precipitator, where it was in the state of fine powder. This reinforcement could not be incorporated into Al 4032 at its melting temperature of nearly 700°C, because of its impermeable nature. Hence, various castings were prepared by increasing the temperature of the furnace gradually and finally at the temperature of 900°C, the reinforcement started to embed in the molten metal, until which, it could be observed on the surface of the molten metal. The furnace was preheated for 30 minutes at a temperature of 900°C [39]. Al 4032 was cut in to pieces and the required proportion of it was introduced in to a crucible made of graphite already in the furnace and the system was maintained at 900°C. The reinforcement was pre heated to 250°C to eliminate moisture contained in it and was transferred to the crucible in the required wt.%. The completed mixture was stirred at 200-300 rpm by adjusting the height of the stirrer such that spilling of the material was avoided. The process of stirring was performed for 3-5 minutes depending upon the wt.% of coal ash. Magnesium in the required proportions was added to increase adhesion between the matrix and reinforcement material. Degassing tablets and coverall fluxes were used to remove entrapped gases and to eliminate to a reaction of the heated metal with atmospheric air. The slag formed on the top of the metal because of reaction of the escaped gases with ambient air was removed periodically. The final mixture was poured into a permanent cast iron mould, pre heated to a temperature of 450°C and the castings were prepared. These castings were cut as per the required dimensions. SEM and XRD analyses were conducted on the prepared samples after following standard procedure to ensure the distribution and presence of reinforcement and are shown in Figures 2(a-d), 3 and 4. Spot EDX was performed on the cast composites to ensure the presence of reinforcement and the results are shown in Figures 3 and 4.

### Vickers micro hardness test

This test is dedicated for finding the surface hardness of the specimens. From each composite produced with various wt. % (0, 2, 4, 6) of reinforcement, one sample was selected for testing. The surface of the selected samples was grinded with emery papers and further polished on a polishing machine to make the surfaces highly polished for testing in a Vickers micro hardness testing machine as per ASTM E10-07 standards. Each sample was loaded with 200 g and applied for a dwell time of 15 s. Five random locations were selected by maintaining a minimum distance between

the locations and the test was conducted to obtain the average value of hardness.

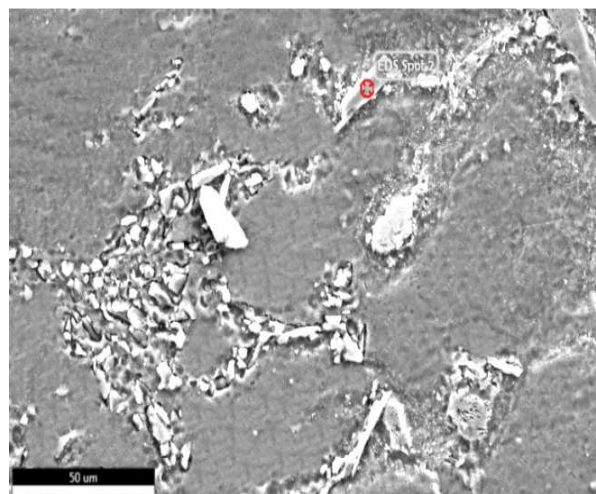


Fig. 3. EDX of composite with 2 wt.% of coal ash

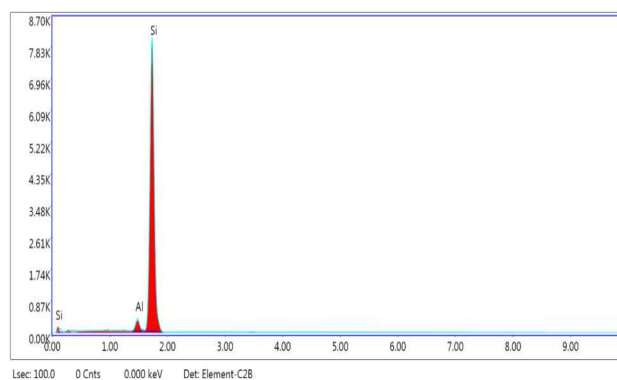


Fig. 4. EDX spectrum of composite with 2 wt. % of coal ash

### DOE and wear test

Wear samples of 25x5x5 mm were prepared from the cast composites with the required wt. % of coal ash to conduct wear tests as per G99 standards.

Based on the literature survey, the reinforcement (wt. %), speed (rpm) and load (N) were identified as the prominent factors. Hence, the control factors considered along with their considered levels are given in Table 4.

TABLE 4. Control factors and their levels

Control factors	Unit	Level			
		1	2	3	4
Reinforcement	[wt.%]	0	2	4	6
Speed	[rpm]	100	300	500	700
Load	[N]	10	20	30	40

Taguchi  $L_{16}$  OA was utilized for the design of experiments so as to decrease the time and expenditure associated with experimentation. The wear test was performed on the prepared samples under dry conditions at room temperature using a pin-on-disc tribometer with a disk made from EN 32 steel with a sliding distance of

1.5 inches. The experiment was conducted under the conditions as per the orthogonal array for 3600 s and the amount of thickness lost was recorded to calculate the wear rate. The experimental conditions and corresponding wear rate are shown in Table 5.

TABLE 5. Experimental conditions and wear rate

Input parameters		Output parameters		
Experiment number	Reinforcement [wt.%]	Speed [rpm]	Load [N]	Wear rate [ $\mu\text{m/s}$ ]
1	0	100	10	1.180
2	0	300	20	1.666
3	0	500	30	2.373
4	0	700	40	3.420
5	2	100	20	1.231
6	2	300	10	1.300
7	2	500	40	2.623
8	2	700	30	3.010
9	4	100	30	1.105
10	4	300	40	1.600
11	4	500	10	1.800
12	4	700	20	2.312
13	6	100	40	1.210
14	6	300	30	1.423
15	6	500	20	1.814
16	6	700	10	2.161

## RESULTS AND DISCUSSIONS

### EDX analysis

EDX analysis was carried out on the produced composites to identify the presence of the coal ash particles. Figures 3 and 4 show the EDX of composite with 2% wt. of coal ash. The reinforced particles are clearly visible in the EDX as shown in Figure 3 and the high peaks of silicon in Figure 4 signify the presence of CA particles.

### SEM analysis

SEM analysis was carried out on the composites as well as on Al 4032 to study the influence of the reinforcement on grain structure and is shown in Figure 2(a-d). Figure 2a corresponds to Al 4032 and Figure 2(b-d) corresponds to the composites with 2, 4, 6 wt.% of coal ash and which reveals the presence of the reinforcement in the matrix material. There were chances for the formation of brittle phases like Al-Ti and Al-Fe, but the proportion of these phases was very low as the maximum amount of coal ash considered was 6 wt.%. Moreover, this addition increased the hardness of the composite, though did not increase the brittleness, which can be observed from the mechanical properties. Furthermore, the presence of the reinforcement created additional nucleation near the rein-

forcement and the average size of the grains was reduced with the increase in wt.% of the reinforcement. The average grain size was measured using ImageJ software and is shown in Table 6. The presence of the reinforcement can also be observed from the change in the morphology of the grains. Uniform distribution of the reinforcement was observed as shown in Figure 2d, which resulted in enhanced strength of the composites.

TABLE 6. Average grain size of composites

S.No	Matrix	Reinforcement	wt.%	Average grain size of matrix phase [ $\mu\text{m}$ ]
1	Al	Nil	0	42.06
2	Al	coal ash	2	34.15
3	Al	coal ash	4	32.32
4	Al	coal ash	6	30.77

### Vickers micro hardness test

This test was conducted on prepared composite specimens to examine the surface hardness of the produced composites and the average value for five locations is shown in Table 7. The values of the micro hardness have increased with the increase in wt.% of the reinforcement. The increase in hardness was attributed to the decrease in spacing between the coal ash particles with the increase in its wt.%. The improvement in the hardness with the wt.% of reinforcement is presented in the Figure 5. The increase in the hardness of the composites was attributed to the addition of hard coal ash reinforcement with a high silicon content to the ductile matrix material. In addition to this, refinement of the grains and reduction in the grain size of the matrix material because of the incorporation of coal ash led to improvement in the strength of the composites, by enhancing the surface area-to-volume ratio of the grains, thereby increasing the resistance to dislocations.

TABLE 7. Results of Vickers hardness test

S.No	Matrix	Reinforcement	wt. %	HV
1	Al	Nil	0	80.96
2	Al	coal ash	2	83.89
3	Al	coal ash	4	85.68
4	Al	coal ash	6	91.79

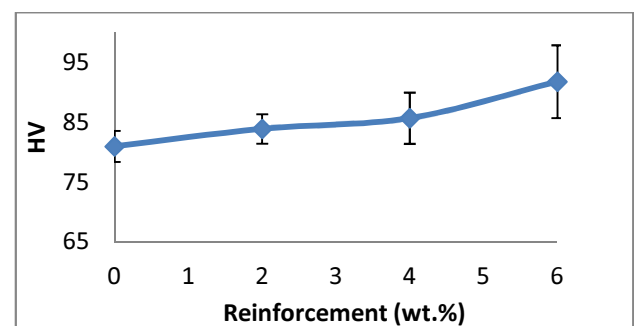


Fig. 5. Variation in Vickers micro hardness (HV) with respect to reinforcement

**Statistical analysis**

The Taguchi method was adopted to design the experiments and study the optimal combination of input parameters on the response. The Taguchi method uses the Signal-to-Noise ratio (S/N) as an objective function to analyze the results. In the present study the smaller the better characteristic was chosen to optimize the wear rate.

**Analysis of factors**

In order to analyze the consequence of individual factors on the wear rate, the S/N values for all the experiments are needed, which were calculated by means of the statistical software Minitab. The lower the better characteristic was employed to calculate the S/N, as the objective was to minimize the wear rate.

The influence of the factors in the order of their effect on the wear rate can be studied from the delta values obtained from the response tables as shown in Tables 8 and 9. From these response Tables, it was observed that speed with the highest rank is the major influencing factor on the wear rate, followed by load and reinforcement.

TABLE 8. Response values of means for wear rate

Level	Reinforcement [wt.%]	Speed [rpm]	Load [N]
1	2.16	1.182	1.61
2	2.041	1.497	1.756
3	1.704	2.152	1.978
4	1.652	2.726	2.213
Delta	0.508	1.544	0.603
Rank	3	1	2

TABLE 9. Response values of S/N for wear rate

Level	Reinforcement [wt.%]	Speed [rpm]	Load [N]
1	-6.014	-1.441	-3.879
2	-5.508	-3.465	-4.673
3	-4.334	-6.54	-5.252
4	-4.146	-8.556	-6.199
Delta	1.868	7.115	2.32
Rank	3	1	2

The main effect plots are also used to analyze the factors and their levels that affect the response. From Figures 6 and 7, it was observed that speed has the most influencing effect followed by load and reinforcement and the optimal parameters obtained for the minimum wear rate are level 4 for reinforcement (6 wt.%), level 1 for speed (100 rpm) and level 1 for load (10 N). It is also evident from Figures 6 and 7 that speed was the major influencing factor, followed by load and reinforcement.

Speed, being most influencing factor on the wear rate, when varied from 100-700 rpm, for all the loads between 10-40 N, the wear rate increased for all the

composites with 0, 2, 4, 6 wt.% of reinforcement and the variation in the wear rate with speed is shown in Figure 8. It was observed that as speed increases, the harder surface of the disc ploughs the surface of the specimens to a deeper extent and is evident as shown in Figure 9(a-b). The worn surfaces underwent severe plastic deformation as the temperature between the rubbing surfaces escalates with the increase in speed and load because of a surge in friction, leading to the formation of debris, grooves and finally leading to ploughing of the material, as observed in Figure 9(a-b).

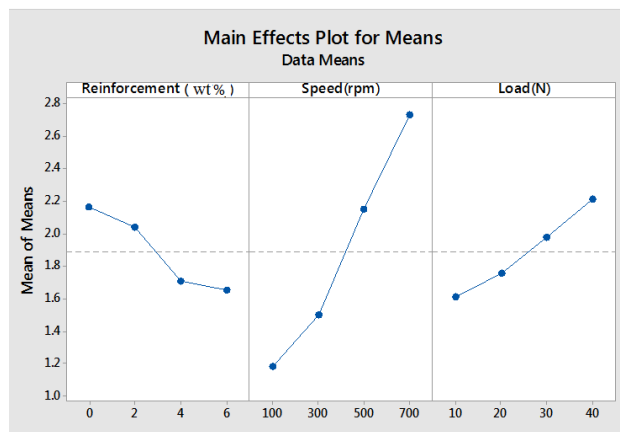


Fig. 6. Main effect plot for means

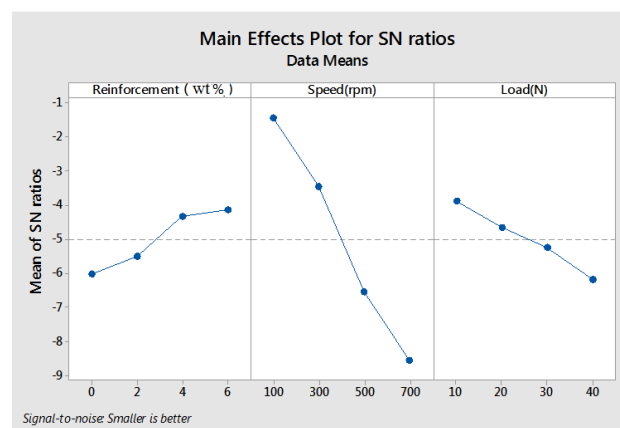


Fig. 7. Main effect plot for S/N

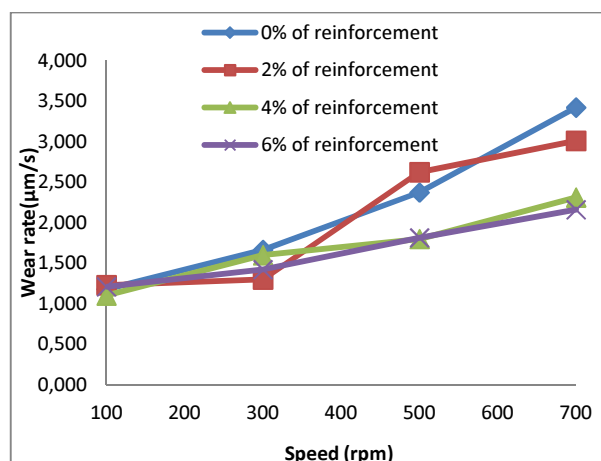


Fig. 8. Variation of wear rate [µm/s] with speed [rpm]

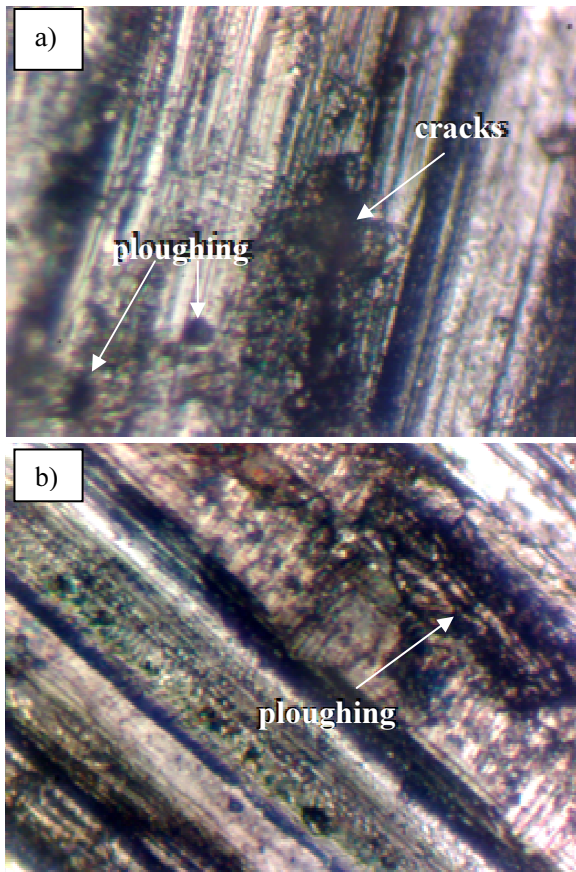


Fig. 9. Optical microscope micrographs of surfaces after wear test of: a) composite with 2 wt.% of CA at 300 rpm and 10 N, b) composite with 4 wt.% of CA at 700 rpm and 20 N

This phenomenon is similar to the observations of several researchers. At higher speeds and loads the stress concentration increased, which initially removed material from the specimen in the form of small particles, leading to the formation of cracks. This effect

increased with the increase in speed as well as load, ultimately causing delamination along with ploughing of the material.

The parallel lines in the interaction plot indicate the absence of a relation between the variables and non-parallel lines signify the effect of a relation between the variables. From Figure 10, it can be seen that there is considerable interaction between the reinforcement and speed on the wear rate at all ranges of speed. This effect was more at high speeds as higher reinforcement wt. % tends to offer more resistance to wear as the speed increases and finally ploughing took place leading to more removal of the material.

A similar phenomenon took place with respect to load, and a significant interaction was observed between the reinforcement and load in Figure 9. The interaction between speed and load was insignificant as the lines are almost parallel.

Figure 11(a, c, e) shows 3D surface plots and Figure 10(b, d, f) shows 2D contour plots of the input variables on the wear rate. The influence of speed and load on the wear rate is shown in Figure 10(a, b). In Figure 10(b), the light green colour represents the minimum wear rate and the dark green color represents the maximum wear rate. The minimum wear rate was observed at low load and minimum speed and it increased with the increase in load and speed. Figure 10(c, d) shows the influence of reinforcement and load on the wear rate. In the Figure 10(d), the blue colour represents the minimum wear rate and dark green colour represents the maximum wear rate. It was observed that the wear rate has decreased with the increase in wt.% of reinforcement and increased with the increase in load. The minimum wear rate was observed at 6 wt.% of coal ash at a load of 10 N and maximum rate of wear was observed at 0 wt.% of coal ash at 40 N.

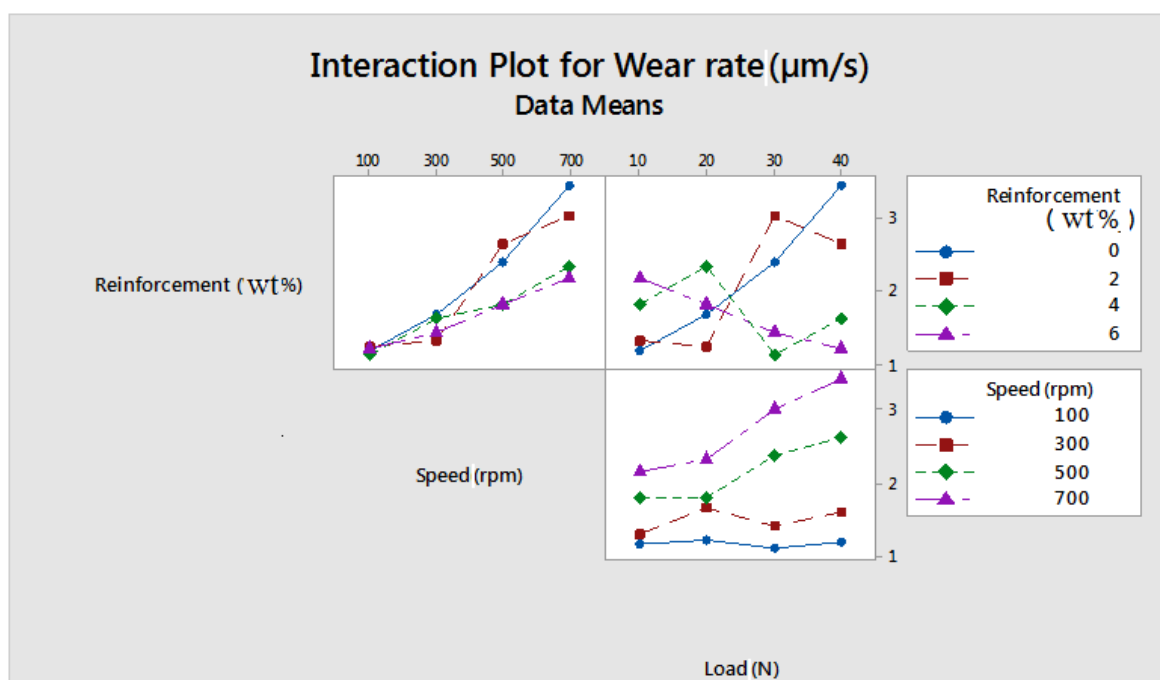


Fig. 10. Interaction plot for wear rate [ $\mu\text{m/s}$ ]

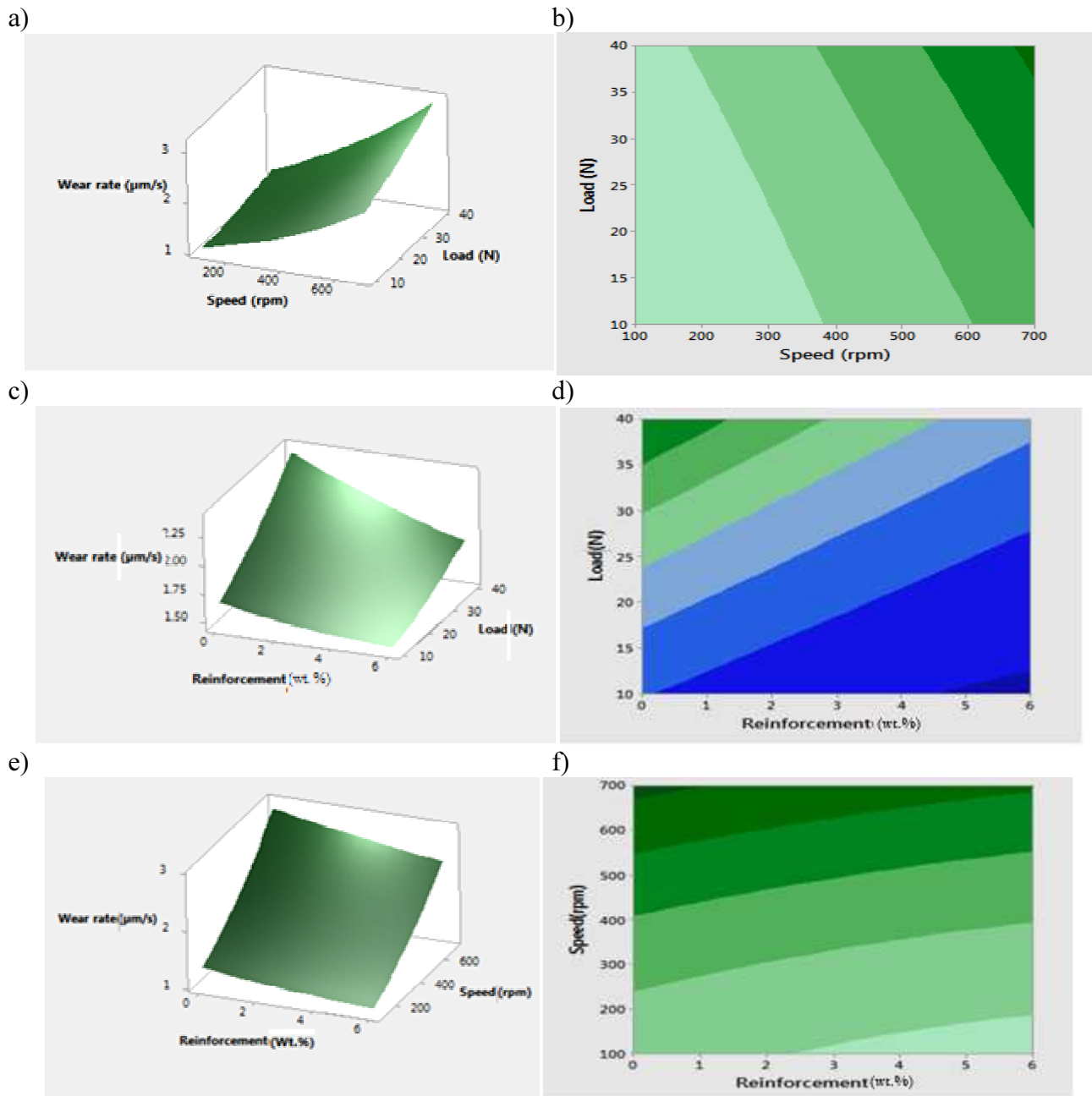


Fig. 11. 3D surface plots (a, c, e), 2D contour plots (b, d, f)

The effect of reinforcement and speed on the wear rate is shown in Figure 11(e, f). In Figure 11(f), the light green colour represents the minimum wear rate and the dark green colour represents the maximum wear rate. It was observed that the wear rate decreased with the increase in wt.% of reinforcement and increased with the increase in speed. The minimum wear rate was observed at 6% wt of coal ash at 100 rpm and the maximum wear rate was observed at 0 wt.% of coal ash at 700 rpm.

#### ANOVA analysis

ANOVA was performed to analyze the significance of the input variables on the wear rate. Table 10 shows the results, indicating speed with 76.10% as the most prominent parameter followed by load and reinforce-

ment with 11.23% and 9.42% respectively, with an R-Sq value of 98.70%. For 95% CI, the effect of square and 2-way interaction were insignificant as observed in Table 10.

#### Regression analysis

A polynomial of the second order was used to represent the wear rate in an un-coded form and is shown as

$$\begin{aligned} \text{Wear rate}(\mu\text{m/s}) = & 1.070 - 0.0110 \text{ Reinforcement} \\ & [\text{wt.}\%] + 0.000436 \text{ Speed} [\text{rpm}] - 0.0008 \text{ Load} [\text{N}] \\ & + 0.00416 \text{ Reinforcement} [\text{wt.}\%] * \text{Reinforcement} \\ & [\text{wt.}\%] + 0.000002 \text{ Speed} [\text{rpm}] * \text{Speed} [\text{rpm}] + \\ & 0.000225 \text{ Load} [\text{N}] * \text{Load} [\text{N}] - 0.000054 \text{ Reinforce-} \\ & \text{ment} [\text{wt.}\%] * \text{Speed} [\text{rpm}] - 0.00212 \text{ Reinforce-} \\ & \text{ment} [\text{wt.}\%] * \text{Load} [\text{N}] + 0.000036 \text{ Speed} [\text{rpm}] * \text{Load} [\text{N}] \end{aligned}$$

TABLE 10. ANOVA results

Source	DF	Seq SS	Adj SS	Adj MS	F-Value	P-Value	Contribution
Reinforcement [wt.%]	1	0.69192	0.10439	0.10439	6.55	0.043	9.42%
Speed [rpm]	1	5.59259	1.69438	1.69438	106.36	0.000	76.10%
Load [N]	1	0.82499	0.23717	0.23717	14.89	0.008	11.23%
Reinforcement [wt.%]*Reinforcement [wt.%]	1	0.00442	0.00442	0.00442	0.28	0.617	0.06%
Speed [rpm]*Speed [rpm]	1	0.06631	0.06631	0.06631	4.16	0.087	0.90%
Load [N]*Load [N]	1	0.0081	0.0081	0.0081	0.51	0.503	0.11%
Reinforcement [wt.%]*Speed [rpm]	1	0.00415	0.00415	0.00415	0.26	0.628	0.06%
Reinforcement [wt.%]*Load [N]	1	0.01586	0.01586	0.01586	1	0.357	0.22%
Speed [rpm]*Load [N]	1	0.04482	0.04482	0.04482	2.81	0.144	0.61%
Error	6	0.09558	0.09558	0.01593			1.30%
Total	15	7.34874					100.00%

S = 0.126; R-sq = 98.70%; R-sq(adj) = 96.75%

DF = degrees of freedom; Seq SS = sequential sums of squares; Adj SS = adjusted sums of squares; Adj MS = adjusted mean squares

All the coefficients with a positive value tend to the increase in wear rate and coefficients with a negative value tend to decrease the value of the wear rate. It was observed from the normal probability plot as shown in Figure 12 that residuals are distributed normally along the straight line for 95 % CI. Multi response prediction was conducted to obtain the optimum parameters for the minimum wear rate and is shown in Figure 13. It was found that reinforcement of 6 wt.%, at the speed of 100 rpm and load of 22.12 N are the optimal parameters for the minimal wear rate.

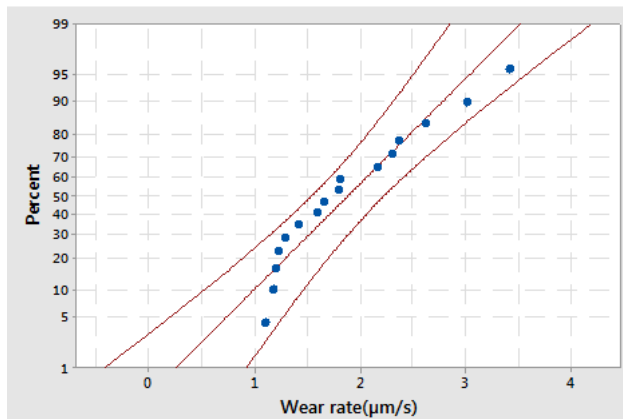


Fig. 12. Normal probability plot

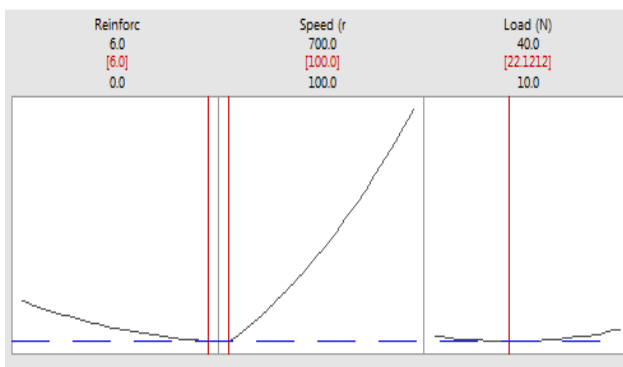


Fig. 13. Results of response optimizer

## CONCLUSIONS

Wear tests were conducted on the composite fabricated by reinforcing Al 4032 with 2, 4, 6 wt.% of coal ash under dry conditions at room temperature as per the Taguchi  $L_{16}$  orthogonal array and the following conclusions were drawn:

1. Composites were successfully fabricated by reinforcing Al 4032 with 2, 4, 6 wt.% of coal ash using the stir casting technique.
2. The presence of coal ash reinforcement in Al 4032 was confirmed using EDX analysis.
3. The distribution of the coal ash reinforcement was analyzed using SEM micrographs revealing uniform distribution of the reinforcement.
4. The optimal parameters obtained for the minimum wear rate from main effect plot were reinforcement with 6 wt.%, the speed of 100 rpm and load of 10 N.
5. ANOVA revealed that speed, with 76.10%, was the most prominent parameter, followed by load and reinforcement with 11.23% and 9.42%, respectively.
6. The normal probability plot revealed that residuals are distributed normally along the straight line for 95% CI.
7. Reinforcement with 6 wt.%, at 100 rpm and 22.12 N are the optimal parameters for the minimal wear rate as optimized from the response optimizer.

## Acknowledgements

Financial support from the Science and Engineering Research Board (SERB) under the young scientist scheme allotted to Dr. Lingaraju Dumpala of JNTUK, Kakinada (SB/FTP/ETA-284/2012) and the AICTE (RPS) Project (File no. 8-188/RIFD/RPS (POLICY-1))/2019-19 is gratefully acknowledged.

## REFERENCES

- [1] Katrenipadu S.P., Gurugubelli S.N., Regression modelling on wear behaviour of nano fly ash-aluminium alloy matrix composites, Emerging Materials Research 2019, 8(3), 418-425.

- [2] Gudimetla A., Sambhu Prasad S., Lingaraju D., Tribological studies of aluminium metal matrix composites with micro reinforcements of silicon and silicon balloons, *Materials Today: Proceedings* 2019, 18, 1, 47-56.
- [3] Doychak J., Metal-and intermetallic-matrix composites for aerospace propulsion and power systems, *JOM* 1992, 44(6), 46-51.
- [4] Trumper R.L., Metal matrix composites: applications and prospects, *Metals and Materials* 1987, 3(11), 662-667.
- [5] Geiger A.L., Walker J.A., The processing and properties of discontinuously reinforced aluminum composites, *JOM* 1991, 43.
- [6] Lingaraju D., Ramji K., Devi M.P., Lakshmi U.R., Mechanical and tribological studies of polymer hybrid nanocomposites with nano reinforcements, *Bulletin of Materials Science* 2011, 34(4), 705.
- [7] Kumar S., Balasubramanian V., Developing a mathematical model to evaluate wear rate of AA7075/SiCp powder metallurgy composites, *Wear* 2008, 264(11-12), 1026-1034.
- [8] Rengasamy N.V., Rajkumar M., Senthil Kumaran S., Mining environment applications on Al 4032-ZrB<sub>2</sub> and TiB<sub>2</sub> in-situ composites, *Journal of Alloys and Compounds* 2016, 658, 757-773.
- [9] Mahendra K.V., Radhakrishna K., Castable composites and their application in automobiles, *Proceedings of the Institution of Mechanical Engineers, Part D, Journal of Automobile Engineering* 2007, 221(1), 135-140.
- [10] Sannino A.P., Rack H.J., Dry sliding wear of discontinuously reinforced aluminum composites: review and discussion, *Wear* 1995, 189(1-2), 1-19.
- [11] Rohatgi P.K., Weiss D., Gupta N., Applications of fly ash in synthesizing low-cost MMCs for automotive and other applications, *JOM* 2006, 58(11), 71-76.
- [12] Ma T., Yamaura H., Koss D.A., Voigt R.C., Dry sliding wear behavior of cast SiC-reinforced Al MMCs, *Materials Science and Engineering: A* 2003, 360(1-2), 116-125.
- [13] Bauri R., Surappa M.K., Sliding wear behavior of Al-Li-SiCp composites, *Wear* 2008, 265(11-12), 1756-1766.
- [14] Jha N., Badkul A., Mondal D.P., Das S., Singh M., Sliding wear behaviour of aluminum syntactic foam: A comparison with Al-10 wt.% SiC composites, *Tribology International* 2011, 44(3), 220-231.
- [15] Tyagi R., Synthesis and tribological characterization of in situ cast Al-TiC composites, *Wear* 2005, 59(1-6), 569-576.
- [16] Kumar S., Subramanya Sarma V., Murty B.S., Influence of in situ formed TiB<sub>2</sub> particles on the abrasive wear behaviour of Al-4Cu alloy, *Materials Science and Engineering: A* 2007, 465(1-2), 160-164.
- [17] Mandal A., Murty B.S., Chakraborty M., Wear behaviour of near eutectic Al-Si alloy reinforced with in-situ TiB<sub>2</sub> particles, *Materials Science and Engineering: A* 2009, 506(1-2), 27-33.
- [18] Prasad D.S., Chintada S., Hybrid composites – a better choice for high wear resistant materials, *Journal of Materials Research and Technology* 2014, 3(2), 172-178.
- [19] Iyer R.S., Scott J.A., Power station fly ash-a review of value-added utilization outside of the construction industry, *Resources, Conservation and Recycling* 2001, 31(3), 217-228.
- [20] Golden D.M., Solidification processing of metal matrix fly ash particle composites, *EPRI Journal* 1994, 46-49.
- [21] Rohatgi P.K., Low-cost, fly-ash-containing aluminum-matrix composites, *JOM* 1994, 46(11), 55-59.
- [22] Baskaran S., Anandkrishnan V., Duraiselvam M., Investigations on dry sliding wear behavior of in situ casted AA7075-TiC metal matrix composites by using Taguchi technique, *Materials & Design* 2014, 1(60), 184-192.
- [23] Li P., Kandalova E.G., Nikitin V.I., In situ synthesis of Al-TiC in aluminum melt, *Materials Letters*, 59(19-20), 2545-2548.
- [24] Tjong S.C., Ma Z.Y., Microstructural and mechanical characteristics of in situ metal matrix composites, *Materials Science and Engineering: R: Reports* 2000, 29(3-4), 49-113.
- [25] Halil A., Ozcatalbas Y., Turker M., Dry sliding wear behavior of in situ Al-Al4C3 metal matrix composite produced by mechanical alloying technique, *Materials & Design* 2006, 27(9), 799-804.
- [26] Sheibani S., Fazel Najafabadi M., In situ fabrication of Al-TiC metal matrix composites by reactive slag process, *Materials & Design* 2007, 28(8), 2373-2378.
- [27] Liu L., Li W., Tang Y., Shen B., Hu W., Friction and wear properties of short carbon fiber reinforced aluminum matrix composites, *Wear* 2009, 266(7-8), 733-738.
- [28] Subrata Kumar G., Saha P., Crack and wear behavior of SiC particulate reinforced aluminium based metal matrix composite fabricated by direct metal laser sintering process, *Materials & Design* 2011, 32(1), 139-145.
- [29] Wang F., Liu H., Yang B., Effect of in-situ TiC particulate on the wear resistance of spray-deposited 7075 Al matrix composite, *Materials Characterization* 2005, 54(4-5), 446-450.
- [30] Kazi Md., Haseeb A.S.M.A., Celis J.P., Tribo-surface characteristics of Al-B<sub>4</sub>C and Al-SiC composites worn under different contact pressures, *Shorowordi, Wear* 2006, 261(5-6), 634-341.
- [31] Ramesh C.S., Pramod S., Keshavamurthy R., A study on microstructure and mechanical properties of Al 6061-TiB<sub>2</sub> in-situ composites, *Materials Science and Engineering: A* 2011, 528(12), 4125-4132.
- [32] Dinaharan I.N., Siva Parameswaran M., Influence of in situ formed ZrB<sub>2</sub> particles on microstructure and mechanical properties of AA6061 metal matrix composites, *Materials Science and Engineering: A* 2011, 528(18), 5733-5740.
- [33] Lingaraju D., Ramji K., Mohan Rao N.B.R., Characterization and prediction of some engineering properties of polymer-clay/silica hybrid nanocomposites through ANN and regression models I.: *Procedia Engineering* 2011, 10, 9-18.
- [34] Basavarajappa S., Chandramohan G., Paulo Davim J., Application of Taguchi techniques to study dry sliding wear behaviour of metal matrix composites, *Materials & Design* 2007, 28(4), 1393-1398.
- [35] Mahapatra S.S., Patnaik A., Study on mechanical and erosion wear behavior of hybrid composites using Taguchi experimental design, *Materials & Design* 2009, 30(8), 2791-2801.
- [36] Prasanta S., Wear behaviour of electroless Ni-P coatings and optimization of process parameters using Taguchi method, *Materials & Design* 2009, 30(4), 1341-1349.
- [37] Koksai S., Fici F., Kayikci R., Savas O., Experimental optimization of dry sliding wear behavior of in situ AlB<sub>2</sub>/Al composite based on Taguchi's method, *Materials & Design* 2012, 42, 124-130.
- [38] Şahin Y., Abrasive wear behaviour of SiC/2014 aluminium composite, *Tribology International* 2010, 43(5-6), 939-943.
- [39] Gudimetla A., Prasad S.S., Lingaraju D., Influence of RHA reinforcements on mechanical and wear behavior of Al 4032 composites, *Emerging Materials Research*, 9(4), 1237-1249.